
This manuscript has been submitted for publication in EARTH AND PLANETARY SCIENCES LETTERS. Please note that this manuscript has not yet undergone peer-review. Subsequent versions of this manuscript may have slightly different content. If accepted, the final version of this manuscript will be available via the “Peer-reviewed Publication DOI” link on the right-handed side of this webpage.

Please feel free to contact any of the authors; we welcome feedback.

Title: Insights into plume-ridge-transform fault interactions as derived from 3D numerical geodynamic modelling of the Azores Triple Junction

Authors:

1. Jaime Almeida (jaime.almeida@segal.ubi.pt, @JaimeEAlmeida1)
2. João Duarte
3. Filipe Rosas
4. Ricardo Ramalho
5. Rui Fernandes

1 Highlights

2 **Insights into plume-ridge-transform fault interactions as derived from 3D numerical geody-** 3 **namic modelling of the Azores Triple Junction**

4 Almeida, J., J. Duarte, F. Rosas, R. Ramalho, R. Fernandes

- 5 • The configuration of the present-day Azores domain is the result of a complex interaction between a
6 ridge, a transform fault and a mantle plume.
- 7 • Due to a shift in tectonic forcing, these interactions promoted the formation of a new intraoceanic rift
8 system.
- 9 • The diffuse nature of the Eurasia-Nubia plate boundary in the Azores can be explained by plume-
10 induced strain delocalization.

11 Insights into plume-ridge-transform fault interactions as derived from 3D
12 numerical geodynamic modelling of the Azores Triple Junction

13 Almeida, J.^{a,*}, J. Duarte^{c,d}, F. Rosas^{c,d}, R. Ramalho^{1,d}, R. Fernandes^a

^a*Instituto Dom Luiz (IDL) - Universidade da Beira Interior, Covilhã, Portugal*

^b*Departamento de Geologia, Faculdade de Ciências da Universidade de Lisboa, Lisbon, 1749-016, Portugal*

^c*Instituto Dom Luiz (IDL) - Faculdade de Ciências da Universidade de Lisboa, Lisbon, 1749-016, Portugal*

^d*School of Earth and Environmental Sciences, Cardiff University, Cardiff, CF10 3AT, UK*

14 **Abstract**

15 The Azores Archipelago is an igneous province located in the centre of the Atlantic Ocean marked by a large
16 bathymetric plateau with a complex tectonic history. Over the last 10 Myr, this region has been shaped
17 by the interaction between the Azores plume, the Mid-Atlantic Ridge (MAR), and the Gloria Fault zone.
18 This complex interaction was characterised namely by the transition from a ridge-ridge-transform (R-R-T)
19 triple junction to a diffuse complex triple zone, with the implied tectonic stresses being accommodated
20 along several right-lateral oblique extensional structures, including the Terceira Rift. An understanding of
21 the main geodynamic mechanisms behind this transition is still lacking.

22 This work explores how the Azores system may have been shaped by these complex plume-ridge-transform
23 fault interactions by running 3D viscoelastoplastic geodynamic models using the LaMEM code. We base
24 our initial modelling setup on previously proposed reconstructions for Azores during the Early Miocene,
25 and implement a complying shift from spreading to right-lateral regional strain rate conditions. We further
26 implemented a plume rising below the MAR to gain additional insight on the nature of the main geodynamic
27 process-interactions governing this system.

Our results suggest that the present-day geometric configuration of the Azores, as well as the formation
of the Terceira Rift, are strongly conditioned by the interactions between plume-ridge-transform fault system
under the right-lateral relative motion between Eurasia and Nubia, as well as by the growth of the Azores
Plateau. Under our modelling conditions, a thicker and weaker Azores Plateau, interfering with a mantle
plume, promotes the localisation of deformation along its edges which act as rheological boundaries. As a
consequence, the global shift in tectonic forcing is shown to be capable of strongly localize strain along the
NE edge of the plateau, closely mirroring the present-day location of the Terceira Rift.

28 *Keywords:* Azores, mantle plume, ridge-plume interactions, geodynamics, numerical modelling

29 1. Introduction

30 The Azores Archipelago is located at the centre of the Northern Atlantic Ocean (Fig. 1) and is the
31 expression of a broad triple zone of distributed deformation (Fig. 1), with the Nubia and Eurasian plates
32 to south- and north-east respectively, and the North American plate to the west. It is also the home of its
33 namesake mantle plume, which has been suggested as a partial source of the volcanism in the region, with
34 the other being the Mid-Atlantic Ridge (MAR) (e.g., [Beier et al., 2022](#)).

35 The Azores plume is a well established and studied feature of this region, from a geophysical (e.g., [Bowin
36 et al., 1984](#); [Silveira et al., 2006](#); [Yang et al., 2006](#); [Pilidou et al., 2005](#)), geochemical (e.g., [Beier et al., 2022](#)),
37 and geodynamic (e.g., [Arnould et al., 2019](#)) point of view. Its exact geometry and location are relatively
38 unclear, varying significantly according to different published works. For instance, using seismic tomography,
39 [Silveira et al. \(2006\)](#) argued that the plume is no longer rooted in the lower mantle, with the characteristic
40 low velocity anomaly being confined mostly to the top 200 km of the upper mantle; while the work from
41 [Yang et al. \(2006\)](#) suggests that the plume stem is rooted below 400 km, and can be traced throughout
42 the upper mantle. The authors further suggest that the plume head is presently located below Terceira
43 Island, which is also in accordance with the studies conducted by [Gente et al. \(2003\)](#). A more recent work,
44 [Arnould et al. \(2019\)](#), explored this region using seismic tomography and argued that this plume is strongly
45 asymmetric. To this extent, they show that the plume has an elliptical shape which spans ca. 2000 km
46 south and 600 km north along the axis of the MAR, and link this shape to the relative motion between
47 the three involved plates and a slight northward drift of the plume itself. While the absolute motion of
48 the plume may be small, reconstruction works conducted by [Beier et al. \(2022\)](#) and [Gente et al. \(2003\)](#)
49 show a more significant relative position change over the past 50 Ma, mostly due to surface tectonic plate
50 reconfigurations. Regarding its influence at the surface, it has been shown that the arrival and spread of
51 the plume below the Azores lithosphere has induced widespread volcanic activity over several million years,
52 being the major contributor to the formation and growth of the Azores Plateau (e.g., [Beier et al., 2022](#)).

53 The Azores Plateau is a small igneous province which is marked by a large bathymetric swell (Fig. 1). It
54 has been proposed to be the result of a two-staged interaction between the Azores plume and the MAR, with
55 the older volcanic materials (> 4 Ma) being mostly plume-related ([Beier et al., 2022](#)), whereas later materials
56 (< 2 Ma) being mostly the result of the rifting processes in the region ([Storch et al., 2020](#); [Beier et al., 2022](#)).
57 It is bisected by the MAR, limited to the south by the East Azores fracture zone (EAFZ) and to the north(-

*Corresponding author.

Email address: jaime.almeida@segal.ubi.pt (Almeida, J.)

58 east) by the Terceira Rift (Fig. 1). The latter represents a NW-SE striking structure connecting the MAR
59 to the western Gloria Fault (GF) zone and presently undergoing ultraslow dextral transtension (e.g., Vogt
60 and Jung, 2004; Fernandes et al., 2006; DeMets et al., 2010; Marques et al., 2013; Weiß et al., 2015; Storch
61 et al., 2020). This transtensional behaviour has been attributed to the relative right-lateral global motion
62 between the Eurasia and Nubia plates (Weiß et al., 2015), which locally induces NW-SE compression and
63 NE-SW extension along this segment of the plate boundary (e.g., Luis and Miranda, 2008; Fernandes et al.,
64 2003; Lourenço et al., 1998).

65 To this day, the geodynamic constraints behind the formation of the Terceira Rift are not fully un-
66 derstood, with different formation mechanisms having been proposed to explain it. The early neotectonic
67 studies on the region (Madeira and Ribeiro, 1990, and references therein) sustained an interpretation of
68 this feature as a "leaky transform", derived from the stress partitioning effect between the right-lateral GF
69 and the spreading at the MAR, resulting in a transtensional component between them (shown in Fig. 8
70 of Madeira and Ribeiro, 1990). Later works regarding bathymetric (Lourenço et al., 1998) and gravimetric
71 (Luis et al., 1998) surveys of the Azores Archipelago agreed with Madeira and Ribeiro (1990) that the Ter-
72 ceira Rift was accommodating extension, but argued that it consisted instead of an extensional strike-slip
73 fault.

74 By compiling gravitational, sediment and plate kinematics data, Gente et al. (2003) suggested that
75 the capture and migration of the Azores plume between 20 and 10 Ma caused the disruption of the Pico-
76 Gloria fault zone (an earlier fault zone which comprised the GF and Pico Fault) and the migration of the
77 plate boundary northwards, creating a weak zone broadly located where the present day Terceira Rift can be
78 found. By contrast, Vogt and Jung (2004) argue that the morphology of the Terceira Rift strongly resembles
79 "hyper-slow" ridges (with spreading rates < 2 mm/yr) around the world. In their view, the Terceira Rift
80 represents the most recent (ca. 1 Ma) of a series of ultra-slow spreading centres formed in this region due
81 to the motion between the Eurasia and Nubia plates. In their numerical modelling study of the mantle
82 dynamics of triple junctions, Geogren and Sankar (2010) use the Terceira Rift as one of the branches of a
83 possible R-R-R Azores Triple junction, albeit while acknowledging that a strike component of motion may
84 exist.

85 Another modelling study, conducted by Neves et al. (2013), used 2- and 3-D elastoplastic models to argue
86 that the broadly NW-SE alignments of volcanic edifices (e.g., the Pico-Faial islands or the Princess Alice
87 basin, Fig. 1), as well as the formation of the Terceira Rift were the consequence of a brittle fracturing pattern
88 developed as the GF propagated towards the MAR. According to the authors, this pattern is controlled by

89 the shearing induced by the GF, by locally variable elastic thickness, and by the drag exerted by the mantle.

90 Using high resolution bathymetry and seismic multichannel data from this region (Weiß et al., 2015)
91 proposed timelines for the formation/development of different features in the Azores Archipelago, which
92 were broadly in agreement with the modelling study by Neves et al. (2013). The work from Weiß et al.
93 (2015) was also found to be in general agreement with the study conducted by Beier et al. (2022), in which
94 bathymetric, seismic, petrological and geochemical data obtained for the archipelago was used to propose
95 a timeline for the growth of the Azores Plateau. In agreement with Neves et al. (2013), both Weiß et al.
96 (2015) and Beier et al. (2022) propose NW-SE oriented fracturing under broadly transtensional conditions,
97 albeit with different timing (e.g., Weiß et al., 2015 shows the formation of the Terceira Rift at 25-20 Ma,
98 while Beier et al., 2022 proposes its formation at 1.5-1 Ma).

99 Among the various proposed formation mechanisms for the Terceira Rift (and other extensional features
100 in the region, such as the Princess Alice Basin or the northern King’s Trough, (e.g., Kidd et al., 1982;
101 Srivastava et al., 1990), one consistent characteristic is the shift in tectonic forcing induced by the Early
102 Miocene right-lateral motion between Eurasia and Nubia (e.g., Potter and Szatmari, 2009; Jolivet and
103 Faccenna, 2000), which resulted in transpressive/transtensive conditions along this plate boundary (e.g.,
104 Hensen et al., 2019). In this work, we use 3D state-of-the-art viscoelastoplastic geodynamic models to
105 simulate the effects of a regional tectonic forcing change in a triple junction setting. To this extent, we use
106 an initial model setup which is broadly based on reconstructions for the Azores system during the Early
107 Miocene (e.g., Gente et al., 2003), simulating a generic oceanic ridge-transform-ridge system in which one
108 of the transform faults is longer and extends further away from the ridge (Fig. 2). Using this setup, we
109 imposed a shift from rift-orthogonal spreading, between North America and Eurasia plates, to right-lateral
110 transcurrent shearing, between Eurasia and Nubia, to assess whether this global plate kinematics change
111 could locally induce the birth of a new dextral transtensional plate boundary. To complement this approach,
112 we also run models in which we include a positive thermal anomaly at the base of the model close to the
113 MAR (Fig. 2A). This induces the formation of a mantle plume, allowing us to explore whether the tectonic
114 reconfiguration that took place in the Azores was essentially the result of global plate kinematics change or
115 if a local mantle plume could have also played a pivotal role in this evolution.

116 The aim of this study is, therefore, to gain new insights on the geodynamic processes and forces that
117 interacted to shape the Azores Triple Junction into its present configuration and, in the process, derive
118 valuable new understanding on how plumes, ridges, and transform faults may interact in 3D/4D to form
119 complex triple junctions. We also aim to understand how rigid entities, such as oceanic plateaus, may

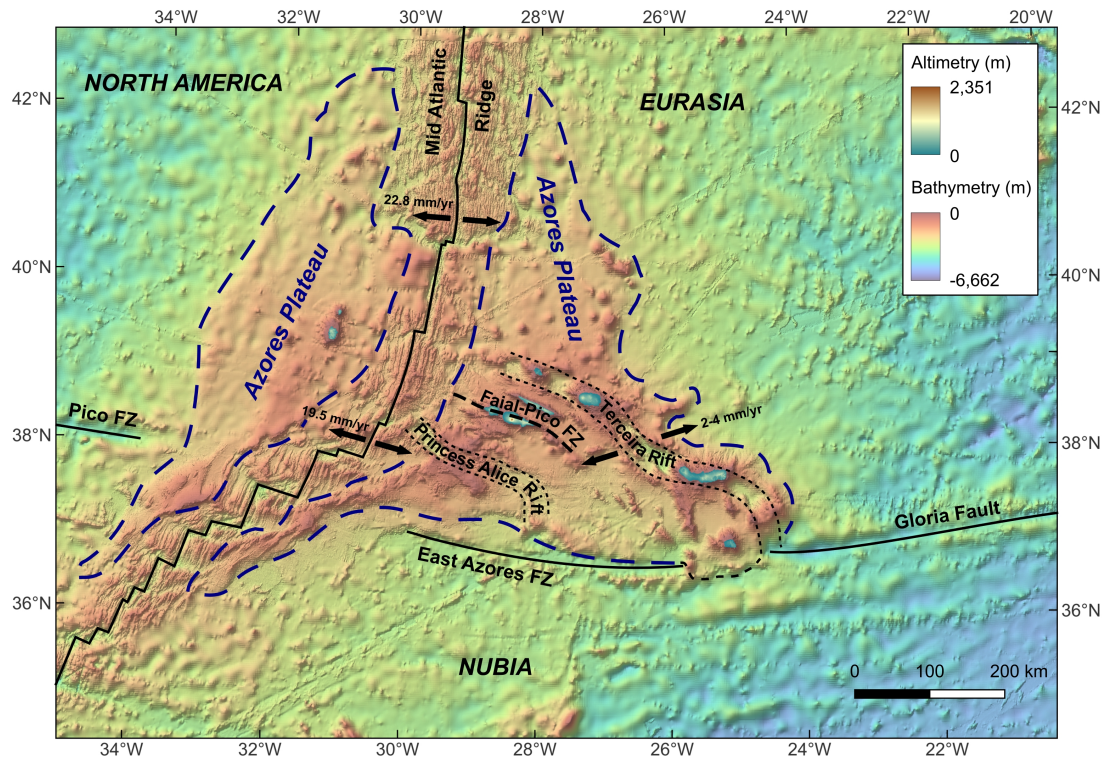


Figure 1: **Overview of the Azores system with the major tectonic features highlighted.** The Azores Plateau is marked by the blue contoured region. The major NE-SW features are highlighted in black lines, with fault zones being marked by thick dashed lines and extensional features being delimited by thin dotted lines. The thick arrows indicate present-day spreading/extensional rates from DeMets et al., 2010. Bathymetry from the EMODnet project (www.emodnet-bathymetry.eu); subaerial topography was generated from a 1:5000 scale digital altimetric database from Secretaria Regional do Turismo e Transportes of the Azores Government. FZ - Fracture Zone

120 influence or condition the geometry and position of ridge jumps and the generation of transtensional diffuse
 121 plate boundaries, such as the one found in the Azores between Eurasia and Nubia.

122 2. Methods

123 2.1. Numerical approach

124 The conducted numerical models were run using the LaMEM code (Kaus et al., 2016), using internally
 125 imposed global strain rate conditions to simulate the seafloor spreading and the shift in tectonic forcing due
 126 to the right-lateral motion between Eurasia and Nubia. No compressibility was assumed for these modelling
 127 runs. LaMEM employs a finite difference staggered grid discretization which is coupled with a particle-in-
 128 cell approach (Kaus et al., 2016) to obtain numerical solutions for the equations of conservation of mass,
 129 momentum, and energy (Eq. 1-3).

$$\frac{\partial \mathbf{v}_i}{\partial x_j} = 0 \quad (1)$$

$$-\frac{\partial P}{\partial x_i} + \frac{\partial \tau_{ij}}{\partial x_j} + \rho \mathbf{g}_i = 0 \quad (2)$$

$$\rho C_p \left(\frac{\partial T}{\partial t} + \mathbf{v}_i \frac{\partial T}{\partial x_i} \right) = \frac{\partial}{\partial x_i} \left(\kappa \frac{\partial T}{\partial x_i} \right) + H_R + H_S \quad (3)$$

Here, \mathbf{v}_i represents the velocity, x_i the cartesian coordinates, P the pressure, τ_{ij} the shear stress, ρ the density, \mathbf{g} the gravitational acceleration, C_p the specific heat, T the temperature, t the time, κ the thermal conductivity, and H_R and H_S represent the radiogenic and shear heating components, respectively. The shear heating component is defined as:

$$H_S = \tau_{ij} (\dot{\varepsilon}_{ij} - \dot{\varepsilon}_{ij}^{elastic}), \quad (4)$$

with $\dot{\varepsilon}_{ij}$ as the total strain rate tensor and $\dot{\varepsilon}_{ij}^{elastic}$ the strain rate imposed by the elastic deformation.

All presented models were run using non-linear viscoelastoplastic rheologies, with the following constitutive equations (Kaus et al., 2016; Piccolo et al., 2020):

$$\dot{\varepsilon}_{ij} = \dot{\varepsilon}_{ij}^{viscous} + \dot{\varepsilon}_{ij}^{elastic} + \dot{\varepsilon}_{ij}^{plastic} = \frac{\tau_{ij}}{2\eta_{eff}} + \frac{\overset{\circ}{\tau}_{ij}}{2G} + \dot{\gamma} \frac{\partial Q}{\partial \tau_{ij}}, \quad (5)$$

$$\overset{\circ}{\tau}_{ij} = \frac{\partial \tau_{ij}}{\partial t} + \tau_{ik} \omega_{kj} - \omega_{ki} \tau_{kj}, \quad (6)$$

$$\omega_{ij} = \frac{1}{2} \left(\frac{\partial v_j}{\partial x_i} - \frac{\partial v_i}{\partial x_j} \right), \quad (7)$$

with η_{eff} as the effective viscosity, $\overset{\circ}{\tau}_{ij}$ the Jaumann objective stress rate, ω_{ij} the spin tensor, G the elastic modulus and Q the plastic flow potential.

The creep viscosity, η_{vs} , is calculated as:

$$\eta_{vs} = \frac{1}{2} A^{-\frac{1}{n}} \times \dot{\varepsilon}_{II}^{\frac{1}{n}-1} \times \exp \left(\frac{E_a + V_a P}{nRT} \right), \quad (8)$$

with A as the diffusive or dislocation pre-exponential factor, n the stress exponent, $\dot{\varepsilon}_{II}$ the second invariant of the strain rate tensor (Eq. 5), E_a the activation energy, V_a the activation volume and R the gas constant.

Plastic creep is ensured by employing a Drucker-Prager yield criterion (Drucker and Prager, 1952):

$$\sigma_Y = C \cos(\phi) + P \sin(\phi), \quad (9)$$

with σ_Y as the yield stress tensor, ϕ the internal friction angle and C the cohesion. The onset of plastic

148 weakening takes place once mantle materials accumulate at least 10% of total plastic strain and this effect
 149 halts after at least 60% of total plastic strain has been accumulated. During softening, the materials' cohesion
 150 and internal friction angles are linearly reduced until they reach 1% of their initial values. The effective
 151 viscosity (η_{eff}) of the individual phases is obtained by calculating the minimum between the calculated
 152 viscoelastoplastic viscosity and the Newtonian viscosity.

153 The age dependence of the thermal profiles of the plates follows the half-space cooling model:

$$T = T_{surface} + (T_{mantle} - T_{surface}) \times erf\left(\frac{y}{\sqrt{Kt}}\right). \quad (10)$$

154 Here, $T_{surface}$ represents the temperature at the surface of the model (273 K), T_{mantle} is the temperature
 155 at the lithosphere-asthenosphere boundary (1523 K), y is the depth, K the diffusivity, and t is the age of
 156 the plate. The effective (rheological) lithosphere thickness throughout the model is set by the 1523 K (1250
 157 °C) isotherm. The upper mantle thermal profile follows the mantle adiabat, with a gradient of 0.5 K/km.
 158 All material densities are temperature and pressure dependent:

$$\rho = \rho_0 + \alpha(T - T_0) + \beta(P + P_0). \quad (11)$$

159 Here, ρ_0 is the density of the material at the reference temperature T_0 , α is the thermal expansibility
 160 and β is the compressibility.

161 2.2. Initial setup and boundary conditions

162 This work was conducted by running 3D viscoelastoplastic numerical models to investigate if the shift in
 163 tectonic forcing caused by the onset of right-lateral motion between Eurasia and Nubia could have induced
 164 a rearrangement of the R-R-T Azores triple junction, as well as the role played by the Azores plume in this
 165 evolution. This plume influence is evaluated by implementing a corresponding mantle anomaly at the base
 166 of the model. The initial configuration of the model was based on reconstructions of the Azores system
 167 during the Early Miocene, such as the one proposed by [Gente et al. \(2003\)](#). To this extent, we simulate a
 168 ridge-transform-ridge triple junction system, in which the southernmost transform is prolonged away from
 169 the ridge (Fig. 2), bordering the south of the Azores Plateau. To ensure that we assess the individual
 170 effect of each studied parameter, we always modified our models in a systematic manner, changing only one
 171 variable per model run, resulting in a total of 5 models (see Table 1).

172 The prescribed model domain was 1500 km long, 900 km wide and 315 km thick and was discretized
 173 along a 256x256x128 resolution grid. To prevent boundary condition issues, as well as instabilities within

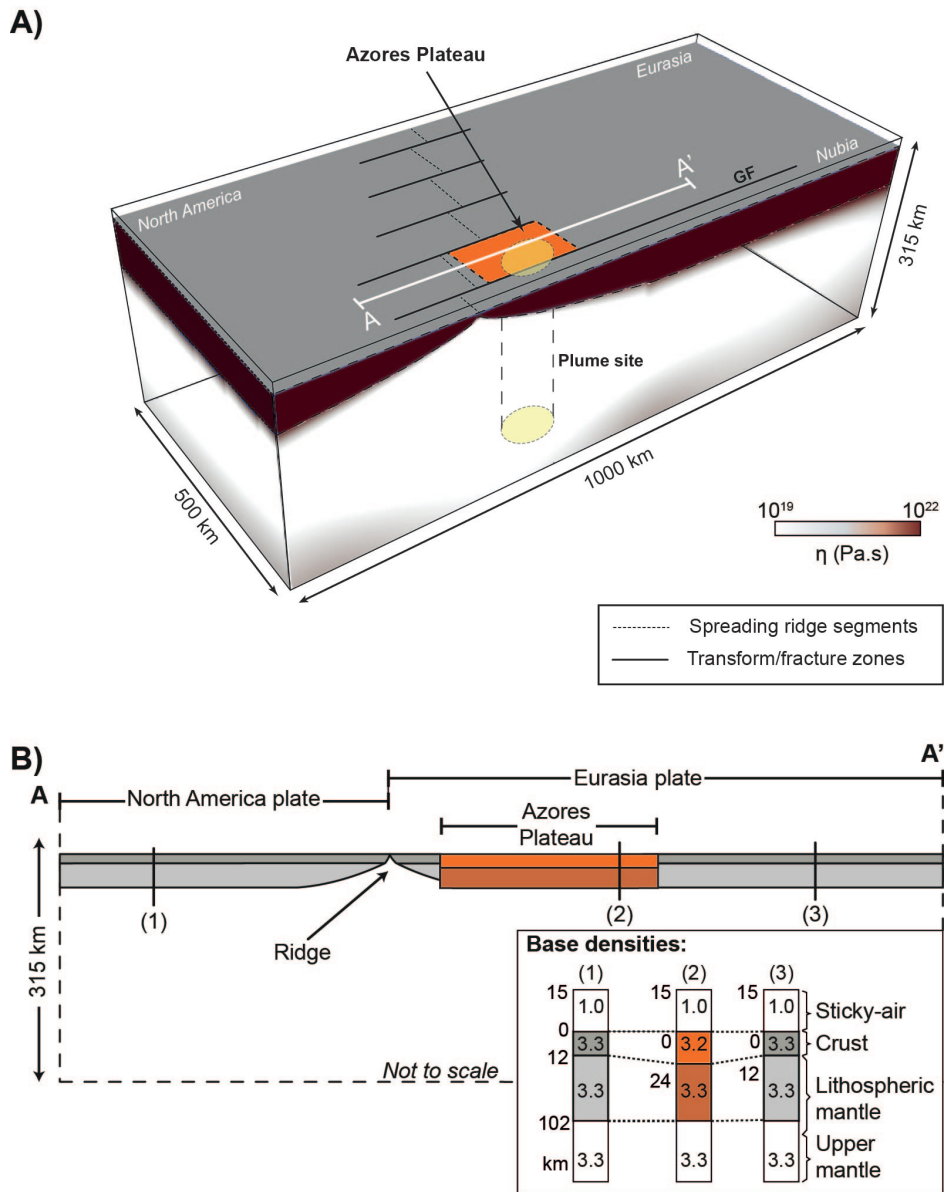


Figure 2: **Initial setup for the conducted models.** **A) Model setup for the experimental initial state:** Schematic representation of the geometric configuration, model dimensions and rheology. The viscosity scale applies to the front- and left-facing wall. To avoid undesired boundary effects due to material accumulation and over stress at the corners of the model, as a consequence of the adopted shear boundary conditions, this region does not correspond to the entire model domain but just a prescribed high resolution domain. **B) Cross section AA' cutting through the Azores Plateau.** Inset shows the initial density structure of the oceanic plates vs. the plateau (units in g/cm^3). Rheologies detailed in the text, and on Supplementary Table S1. GF - Gloria Fault

Table 1: List of models run in the present study. Model 1 (in bold) is considered the reference model.

Model number	Pre-existing plateau	Active plume	Additional constraints
1	Yes	No	-
2	No	No	-
3	No	Yes	No imposed strain rates
4	No	Yes	-
5	Yes	Yes	-

174 the model, this discretization is non-uniform, with a central high-resolution region (shown in Fig. 2A)
 175 surrounded by a low resolution box. The model included a 15 km thick sticky-air layer, which acts as a free
 176 surface, allowing for the formation of topography. Furthermore, the top boundary is open, ensuring a free
 177 movement of this layer. All other model boundaries were defined as free slip, which allows for motion along
 178 the boundary surface but not across it.

179 The rheology of the oceanic crust follows a dry olivine creep law (Ranalli, 1997) and has a variable
 180 thickness which depends on its distance to the spreading ridge (following the half-space cooling model, Eq.
 181 10). The lithospheric mantle also follows a dry olivine creep law, differing in behaviour from the crustal
 182 material due to a higher temperature (Eq. 8).

183 The Azores Plateau was prescribed with a weaker but thicker crust to mimic the volcanic nature of this
 184 region, in this case, following a diabase law (Mackwell et al., 1998). To reflect the accumulation of plume-
 185 derived material at the base of the lithosphere, the plateau interrupts the normal plate growth from the ridge,
 186 resulting in a locally thicker lithospheric mantle close to it as is illustrated in the cross-section shown in Fig.
 187 2B. The transform faults are implemented in the models as thin planar bodies with a constant Newtonian
 188 viscosity of 10^{20} Pa·s as to achieve high strain localization within them. All rheological parameters made
 189 available in Appendix Table S1. The Azores plume was prescribed in our models by injecting hotter (ca.
 190 250 K) material through a point in the bottom boundary with a constant rate of 5 cm/yr. The injection
 191 site is 100 km wide and is located approximately below the Azores Plateau (Fig. 2A). The composition of
 192 the plume material is identical to the surrounding upper mantle (see Supplementary Table S1) and ascends
 193 to the surface due to its positive thermal buoyancy. As prior works have argued that the nature of the
 194 plume (i.e., chemical vs. thermal vs. thermochemical) does not influence the dynamics of ridge-plume
 195 interaction (e.g., Ribe et al., 1995), we adopted the simplification of implementing a thermal anomaly at the
 196 lower boundary of our model. Consequently, we obtained a relatively consistently shaped mushroom-shaped
 197 mantle plume throughout all models which allows for a straightforward comparison between them.

198 The dynamics of the system are controlled by a two-phase regionally imposed strain rate (Fig. 3), which

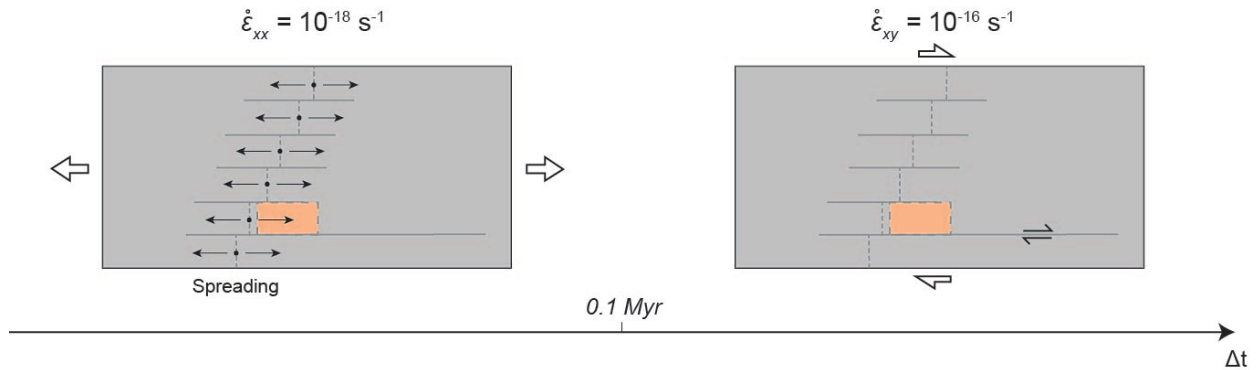


Figure 3: **Top-view illustration of the imposed two-phase regional strain rates, implemented during the entire model evolution.** During a first phase, lasting 100 kyr, the model evolves under regional spreading conditions with a $\dot{\epsilon}_{xx}$ of 10^{-18} s^{-1} . After that, we impose a right-lateral simple shear regional strain rate ($\dot{\epsilon}_{xy}$) of 10^{-16} s^{-1} (corresponding to a right-lateral strike slip velocity of ca. 1 cm/yr), simulating the transcurrent motion of Eurasia and Nubia, which is locally capable of inducing transpressional and transtensional strain in the Azores plateau domain. The large white arrows represent the imposed strain conditions, while the thin black arrows represent the resulting local kinematic conditions.

199 simulates the change in tectonic forcing imposed by the right-lateral motion between the Eurasian and Nubia
 200 plates during the Middle Miocene (e.g., Fernandes et al., 2003; Schettino and Macchiavelli, 2016; Potter and
 201 Szatmari, 2009; Duarte et al., 2013), which is locally capable of triggering transtensional and transpressive
 202 strain in the Azores plateau domain. As we cannot be sure on the exact magnitude of strain during the
 203 Miocene, we adopted the simplification of considering a strain rate equivalent to the one observed in the
 204 Present day (closely corresponding to the ca. 1 cm/yr strike-slip velocity between Eurasia and Nubia). The
 205 models are ran for 100 kyr under regional spreading conditions to ensure the establishment of the MAR and
 206 the initiation of the mantle upwelling beneath the ridge, followed by a regional simple shear component with
 207 $\dot{\epsilon}_{xy} \approx 10^{-16} \text{ s}^{-1}$, which locally induces transpressional and transtensional strain conditions in the Azores
 208 plateau domain. This specific strain rate value was chosen to ensure that the right-lateral motion in the
 209 region reflects the known Eurasia-Nubia relative motions.

210 For simplification, our reference conditions include both the Azores Plateau and the shift in regional
 211 strain rate. Although the former did not exist at the time of the change in tectonic forcing (ca. 10 Ma), it
 212 was formed shortly after (e.g., Beier et al., 2022; Weiß et al., 2015) which could be sufficient to significantly
 213 alter the local rheology contrasts.

214 3. Results

215 3.1. Models without an active mantle plume

216 All models without an active mantle plume showed a similar sequence of events, which is represented in
 217 Fig. 4 and Supplementary Video 1. During the first 100 kyr (Fig. 4A), the MAR is opened, which induces

218 upper mantle upwelling below it (simulating an active mid-ocean ridge). After the prescribed change in the
219 general strain rate regime occurs (Fig. 3), a weak strain localization band is immediately formed (Fig. 4B)
220 connecting the GF and the MAR. As the model evolves (Fig. 4C), this band becomes more localized with
221 its strain rate being two orders of magnitude higher than the background. Once this connection between the
222 GF and the northern segments of the MAR is established, an isolated low strain domain can be observed
223 between these three features (Fig. 4D). This domain is bordered to the north by the newly formed shear
224 zone, which acts as a slow transtensional boundary. Here, the Eurasian plate is separated into two distinct
225 zones, the "original" Eurasia and the new Azores domain. Although both domains are moving away from
226 the MAR, the NE domain moves ca. 3 mm/yr faster, producing intra-oceanic rifting that evolves into a
227 slow spreading centre (Fig. 5).

228 In models in which the Azores Plateau was absent (Model 2, Fig. 6 and Supplementary Video 2), we
229 observed that after the main prescribed change in the strain tectonic regime ($\Delta t \approx 100$ kyr), no particular
230 localization of strain occurs, and consequently, no clearly defined shear zone develops. Instead, a large
231 triangular diffuse high strain rate area develops adjacent to the spreading ridge (to the east of the MAR).
232 This increased strain rate area is maintained throughout the entire modelling run, without strong localization
233 ever developing.

234 3.2. Models with an active plume

235 In order to assess the influence which could be exerted by the Azores plume alone, the main strain
236 regimes (and the induced shift between them) that were prescribed in all other models were disabled in
237 Model 3 (Fig. 7A and Supplementary Video 3). Thus, in this model, all observed surface strain is the result
238 of the mantle plume head encroaching at the base of the lithosphere, with a minor contribution from ridge
239 push. Consequently, the strain magnitudes are significantly lower than the ones observed in both Models 1
240 and 2 (as seen in Fig. 7A). During the first ca. 500 kyr, the majority of strain is localized at the MAR and
241 associated weak zones while the plume ascends through the upper mantle. Upon arriving at the base of the
242 lithosphere (600-800 kyr) the plume head temporarily disrupts the MAR by forcefully inducing the opening
243 of two ridge segments (Fig. 7A1). However, as the plume head spreads beneath the lithosphere (0.8-1.1
244 Myr), the two segments are re-established at their initial positions and the surface deformation effects of
245 the plume stop being visible (Fig. 7A2).

246 The regionally imposed strain rates were implemented again in Model 4 (Fig. 7B) in order to assess how
247 the shift in tectonic forcing could enhance or inhibit the surface strain caused by the mantle plume. Under
248 these conditions, we once again observe the same event sequence as in the models without the active plume.

Model 1 (pre-existing plateau, no active plume)

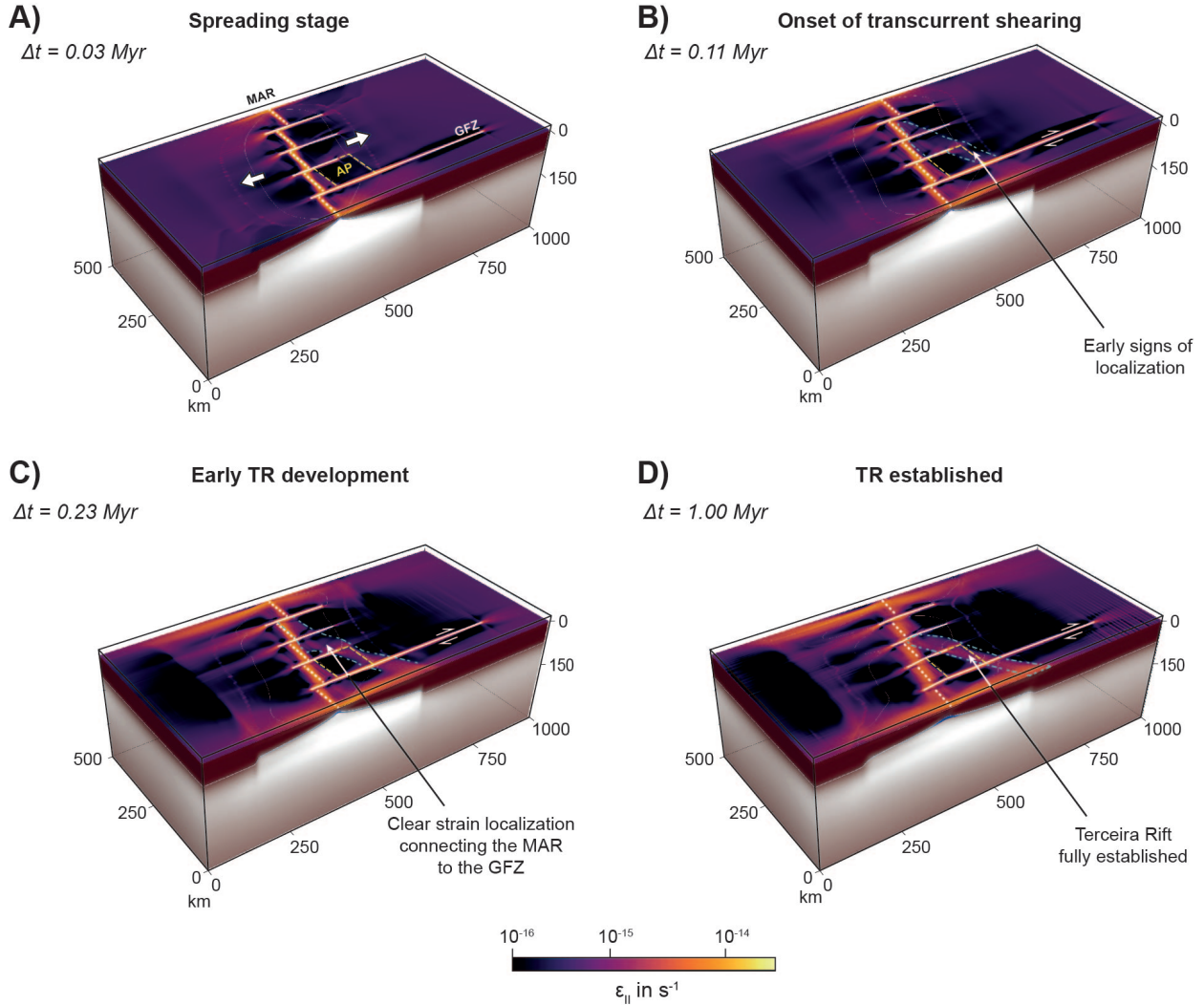


Figure 4: **Evolution of the reference model (Model 1) over 1 Myr.** **A) Spreading phase.** The upwelling of the mantle below the MAR is induced, allowing for the establishment of the weak zones associated with this feature (such as the central valley). **B) Shift in tectonic forcing.** After 100 kyr have elapsed, the regional simple shear conditions are imposed on the model. There is an immediate establishment of a narrow shear zone that localizes transensional strain and connects the GF to the MAR. This also results in the isolation of a small triangular domain between this shear zone, the GF and the MAR. **C) Early development of the TR.** After another ca. 100 kyr, strain localization is further developed, with increased transensional strain and simultaneous narrowing of the forming shear zone. It is also noticeable that the isolated triangular domain is characterized by a low strain rate, implying that the newly formed band is acting as a plate boundary (much like the Terceira Rift). **D) Final deformation state.** After ca. 1 Myr of evolution, the new transensional shear band is fully developed, with a geometry and kinematics compatible with the one observed for the natural Terceira Rift. MAR - Middle-Atlantic Ridge; GF - Gloria Fault; AP - Azores Plateau; TR - Terceira Rift.

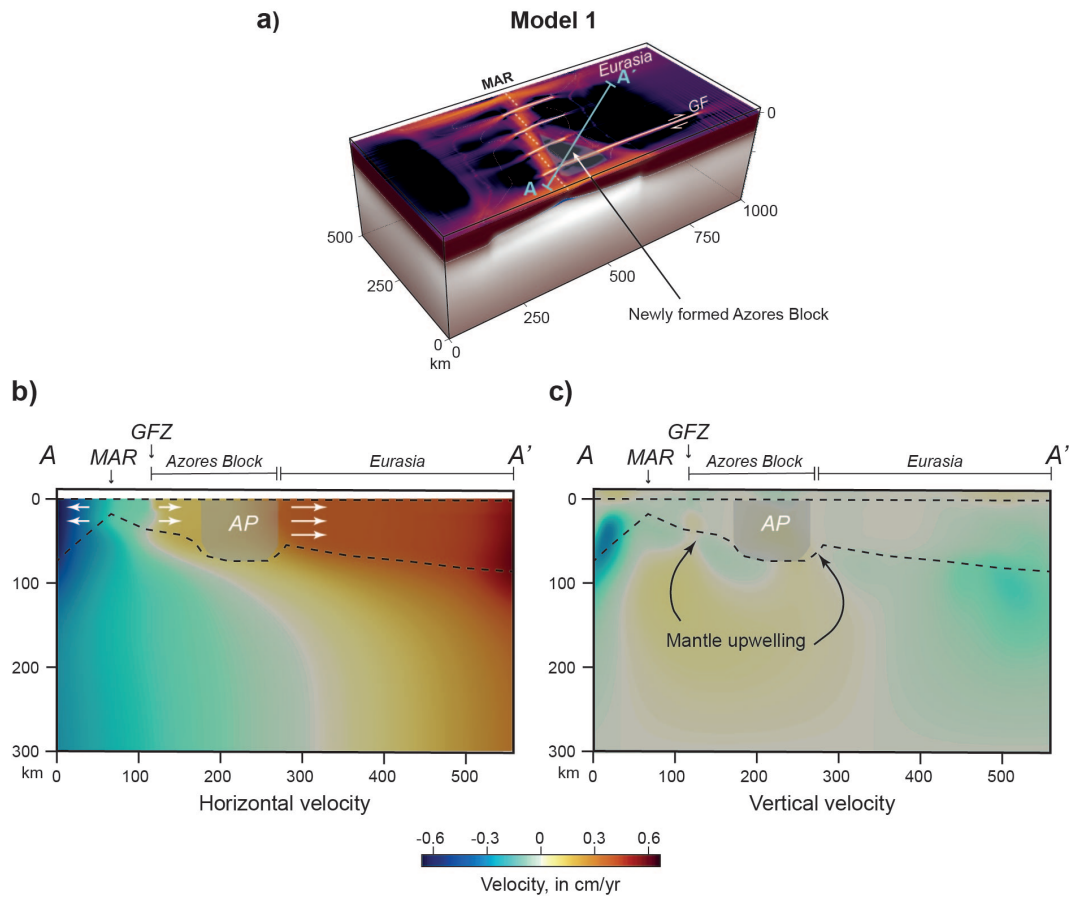


Figure 5: Newly formed transtensional shear zone boundary (corresponding to the Terceira Rift). **A) Model 1 after 1 Myrs, depicting the location of the cross sections orthogonal to the newly formed transtensional shear zone.** **B) Cross section AA': horizontal velocity output.** Note that the horizontal velocity displays a jump in magnitude towards the NE (i.e., to the right) across the newly formed shear zone, denoting marked extensional strain localization along the NE boundary between the triangular Azores Block and the rest of the Eurasia plate. The Eurasia plate has been separated into two separated strong blocks, the "original" Eurasia plate (to the NE), and the new Azores Block domain. While both are moving away from the MAR, the north-eastern Eurasia region is moving ca. 3 mm/yr faster, producing a slow spread along this new boundary. **C) Cross section A-A': viscosity output.** The separation observed in the previous cross-section is accompanied by two small mantle upwelling sites, under the GFZ and the TR-like shear zone, showing some degree of mantle accommodation to the transtensional deformation in the region. MAR - Middle-Atlantic Ridge; GF - Gloria Fault.

Model 2 (no active plume, no plateau)
 $\Delta t = 1.00 \text{ Myr}$

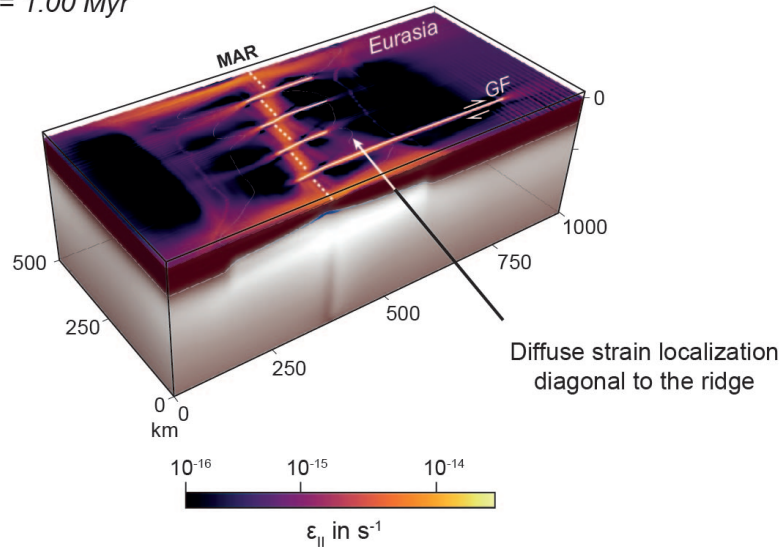


Figure 6: **Final deformation state in Model 2.** Diffuse strain distribution occurs throughout the entire Azores domain (between the GF, the MAR and the Eurasia plate to the NE). MAR - Middle-Atlantic Ridge; GF - Gloria Fault.

249 However, and unlike Model 3, the MAR is never disrupted during plume ascension (see Supplementary
 250 Video 4). Furthermore, a wider high strain rate region is formed in these models when compared to Model
 251 3 (Fig. 7A vs. 7B).

252 Lastly, in Model 5 (Fig. 7C), we added the Azores Plateau to assess how the complete set of geodynamic
 253 constraints would affect the evolution of this system. This model shows the combined features from all the
 254 previous models. We observe a broadly triangular-shaped high strain rate domain bounded by the MAR
 255 and the GF as in Models 1 and 2 (Fig. 4 and 6), without any low strain rate zones being formed.

256 4. Discussion

257 4.1. The effects of the right-lateral motion between Eurasia and Nubia

258 One of the primary objectives of this work was to explore how the change in relative motion between
 259 the Eurasian and Nubian plates (e.g., Weiß et al., 2015) could influence the formation of the Terceira Rift.
 260 To simulate these changes, we begin with an initial setup which is based on geological reconstructions for
 261 the region (Fig. 8A) and simulates the shift from orthogonal rift spreading to dextral simple shear, induced
 262 by the onset of right-lateral strike-slip movement between Eurasia and Nubia plates along the GF. (Fig. 3).
 263 This imposed strain rate regime is induced by the relative right-lateral motion along the GF (e.g., DeMets
 264 et al., 2010; Fernandes et al., 2006), in which Eurasia moves eastwards relative to Nubia. This shift in the
 265 overall governing strain rate regime expresses a reorientation of the regional stress field, with the principal

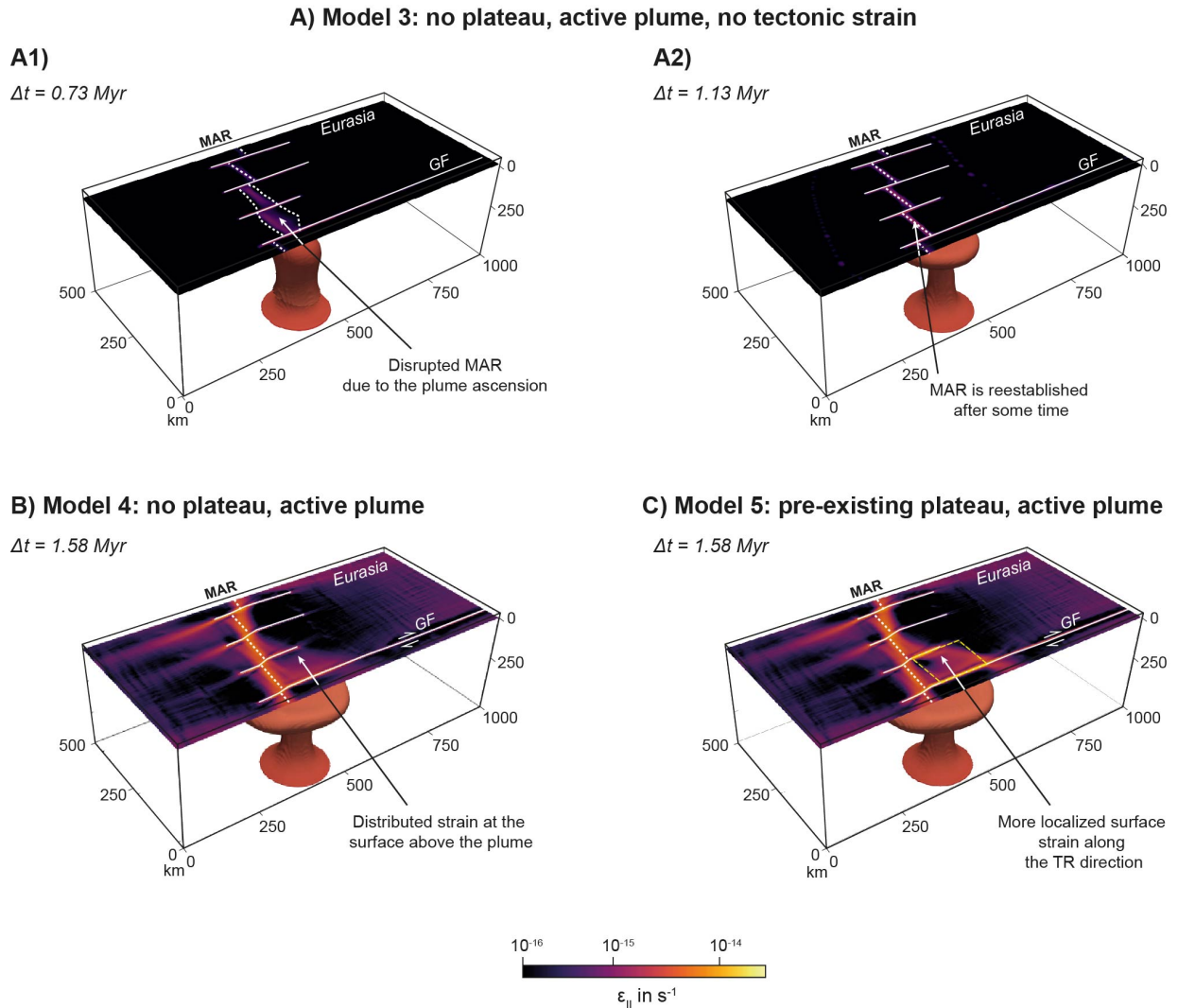


Figure 7: Evolution and final states of the plume models (Models 3 to 5). **A1.** Disruption of the MAR in Model 3. Upon arrival of the plume head to the base of the lithosphere, there is a disruption of the MAR, as illustrated by the broadening of spreading centres in two of the MAR segments. **A2.** Reestablishment of the MAR. Over time, the MAR is reformed in its original position as the result of the lack of regional shearing. **B) and C) Final deformation states in Models 4 and 5.** The arrival of the plume in these models with a pre-imposed regional strain rate shows surface patterns similar to Model 2 (Fig. 6). However, strain distribution is in this case more diffuse, without any significant localization along any narrow shear bands (compare with Fig. 4D). MAR - Middle-Atlantic Ridge; GF - Gloria Fault.

266 extension direction rotating from E-W to NE-SW, compliant with the known NW-SE oriented extensional
267 features, such as the Terceira Rift, the Princess Alice Rift, the King’s Trough (e.g., [Gente et al., 2003](#); [Kidd
268 et al., 1982](#); [Srivastava et al., 1990](#)) and the volcanic alignments in the region (e.g., [Neves et al., 2013](#); [Weiß
269 et al., 2015](#), Fig. 1). We also explored how the presence or absence of the Azores Plateau could influence
270 the evolution of the system. This stems from the overlap between the age of formation for this feature, ca.
271 15-10 Ma (e.g., [Beier et al., 2022](#)), and the acceleration of the orthogonal convergence between these two
272 plates in the Mediterranean region, ca. 15-10 Ma (e.g., [Potter and Szatmari, 2009](#); [Rosenbaum et al., 2002](#);
273 [Jolivet and Faccenna, 2000](#)), which imposes the dextral transcurrent kinematics along the GF.

274 Our models without active mantle plumes (Fig. 4 and 6) allow us to obtain some insights concerning the
275 impact of two geodynamic constraints: the existence of the Azores Plateau and change in tectonic forcing)
276 on the evolution of the Azores system. First and foremost, once the tectonic forcing shift takes place, a
277 strain localization boundary is formed at an $\approx 45^\circ$ angle to the MAR and connects it to the GF. The
278 appearance of this boundary can be linked to NE-SW reorientation of the main extensional direction, which
279 thus facilitates this NW-SE MAR-GF connection. The degree of strain localization south along this new
280 boundary is directly correlated with the presence of the Azores Plateau (compare Fig. 4 and 6), as models
281 ran without this feature more distributed strain rate within the same domain. By contrast, when the plateau
282 is present, most strain is localized along a narrow shear zone (Fig. 4) which forms close to the edge of the
283 plateau. This suggests that the rheologically distinct (see Supplementary Table S1) and thicker plateau
284 crust plays a fundamental role in the evolution of the Azores system. On this, prior works concerning the
285 effects of rheologically distinct bodies on transtensional systems have shown that their edges are prime sites
286 for strain localization due to acting as strong rheological boundaries (e.g., [Calignano et al., 2015](#); [Willis
287 et al., 2019](#)). Additionally, it has been shown that localized bodies with thicker crusts (i.e., weak layers)
288 tend to favour both extensional stresses ([Lynch and Morgan, 1987](#)) and delocalized deformation ([Keppler
289 et al., 2013](#)).

290 Our results suggest that this rheological boundary localization effect may be acting in our models. Under
291 our modelling conditions, despite its inherent weak rheology (see Table S1), the cold nature of the imposed
292 Azores Plateau makes it act as a strong body. This promotes the localization of stress along its boundaries,
293 facilitates the creation of the observed strain shadow zones (compare Figs. 4 and 6) and the shear zone which
294 connects the MAR and the GF (Fig. 4). Over time, this shear zone begins to act as an active transtensional
295 plate boundary in our models, isolating a new triangular domain from the surrounding plates (Fig. 8B).
296 We argue that this isolated area represents the Azores domain (Fig. 8B), which was formed between the

297 Terceira Rift, the MAR and the EAFZ (an older, deactivated segment of the Gloria-Pico Fault, Luis and
298 Miranda, 2008, shown in Fig. 8B). This comparison can be strengthened by the kinematic measurements
299 shown in Fig. 5, namely the ca. 3 mm/yr horizontal difference across this boundary, which is in-line with
300 the magnitude of the slow rifting rates observed for the region which range from ca. 1.5 (e.g., Fernandes
301 et al., 2003, 2004) to 3 mm/yr (e.g., Vogt and Jung, 2004).

302 The evolution of our modelled triple junction from its original R-R-T (Fig. 8A) to the final diffuse
303 R-R-R configuration (Fig. 8B) closely follows plate reconstructions for this region (e.g., Gente et al., 2003;
304 Luis and Miranda, 2008; Beier et al., 2022). This triple junction configuration change due to a change in
305 global tectonic forcing is in-line with prior work which suggested that these features are inherently unstable,
306 constantly adapting and reacting to the existing tectonic stresses (Cronin, 1992). In the present case, a
307 change in global tectonic forcing resulted in the establishment of a new transtensional site which, in time,
308 could evolve into an independent ridge site. Thus, our results suggest that the formation of new intraoceanic
309 rift (or oblique extensional) sites are the result of the local expression of a change in global tectonics.

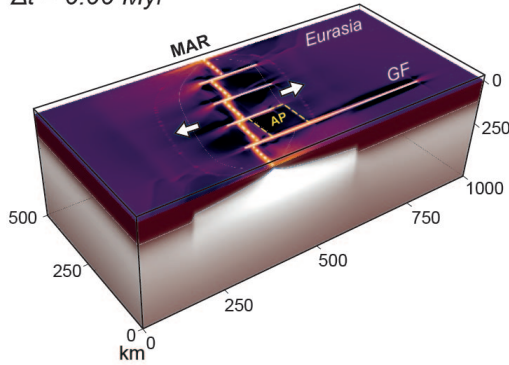
310 4.2. *The mantle plume contribution*

311 Around the world, many plumes are located below or close to mid ocean ridges (Ribe et al., 1995), such
312 as Iceland, Afar, Galapagos or the Azores. This overlap has sparked a plethora of studies in the past which
313 have versed on the interactions between these major geological features (e.g., Ribe et al., 1995; Albers and
314 Christensen, 2001; Pilidou et al., 2005; Mittelstaedt et al., 2011; Gibson et al., 2015; Whittaker et al., 2015;
315 Sun et al., 2021; Pang et al., 2023, among many others). It has been argued that, among other things, plumes
316 can be both captured by ridges (e.g., Schilling, 1991, and references therein) as well as induce new ridge
317 sites (e.g., Whattam and Stern, 2015). They are also known to induce strong geoid and dynamic topography
318 anomalies (e.g., Wang, 2021). Nevertheless, to the best of our knowledge, no modelling study has tackled
319 the combined effects of a ridge-plume-transform interaction triggered by the onset of right-lateral strike-slip
320 motion and its related shearing. As previously shown, our plume head is positioned close to the MAR (Fig.
321 2 and 7), which influences the development of the Terceira Rift in two main ways. First, the arrival of the
322 plume head to the base of the lithosphere induces a temporary disruption of the MAR (i.e., a forced opening
323 of individual segments). Secondly, the edges of the plume head promote the accumulation/localization of
324 strain along specific directions at the surface.

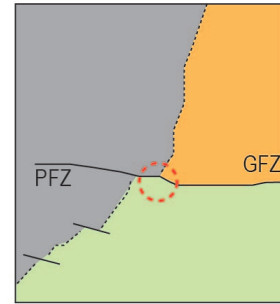
325 We argue that the disruption effect of the MAR, observed in Model 3, represents an attempt at initiating
326 a change in ridge configuration, a process commonly occurring at plume-ridge interaction sites, called a ridge
327 jump (e.g., Mittelstaedt et al., 2011; Gibson et al., 2015; Whittaker et al., 2015). Previous research on this

A) Initial configuration of the triple junction

$\Delta t = 0.00 \text{ Myr}$



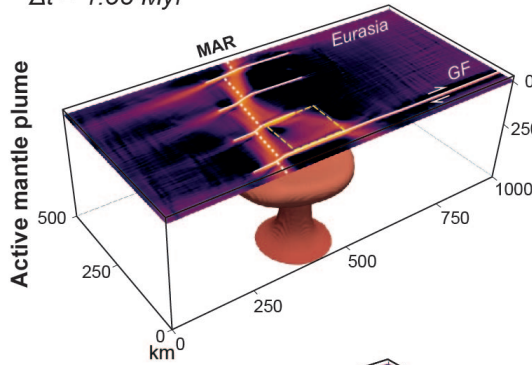
20 Ma



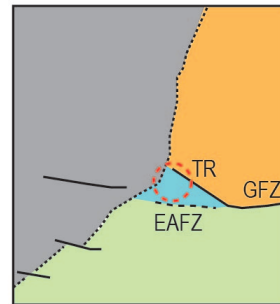
Adapted from Gente *et al.* (2003)

B) Establishment of the Azores domain

$\Delta t = 1.58 \text{ Myr}$



10 Ma



Adapted from Gente *et al.* (2003)

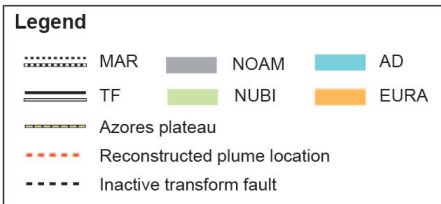
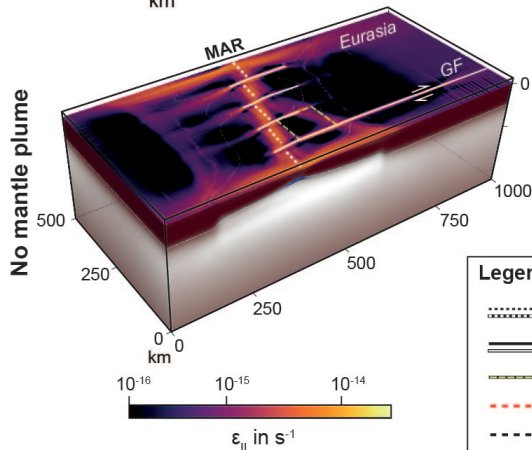


Figure 8: Comparison of the model results with the evolution of the Azores system. **A) Initial configuration of the Azores triple junction.** Our initial setup was based on the reconstructions for the region (such as the one from Gente *et al.*, 2003). During the Early Miocene, the GF was not an isolated fault but instead part of the Pico-Gloria Fault (PF-GF) system. **B) Formation of the Azores domain due to the regional tectonic forcing.** Plate reconstructions for the region propose that the Azores domain (AD) was established in the late Miocene (ca. 10 Ma, Gente *et al.*, 2003) during the tectonic reconfiguration imposed by the relative motion between the Eurasia-Nubia plate (e.g., Potter and Szatmari, 2009). In our results, a similar change from spreading to right-lateral shearing conditions leads to opening of the Terceira Rift, here mimicked by a narrow band of high strain localization which links the MAR to the GF. The deactivation of the EAFZ segment is not simulated in our models due to the simplified implementation of the weak zones as simple isoviscous shapes (a discussion of this can be found in Appendix A - Model Limitations). PF: Pico Fault; GF: Gloria Fault; EAFZ: East Azores Fracture Zone; AP: Azores Plateau; TR: Terceira Rift; NUBI: Nubia plate; EURA: Eurasia plate; NOAM: North America plate; MAR: Mid-Atlantic Ridge; and TF: Transform Fault.

328 topic has suggested that ridge jumps are the result of the coexistence between a weakening of the lithosphere
329 around a mid-ocean ridge and a rift-inducing stress field (Mittelstaedt et al., 2011, and references therein).
330 Under the conditions of Model 3, no ridge jump is observed suggesting that one or both of these factors
331 are not present. Although not visible in Fig. 7A, the encroaching mantle plume induces a small degree of
332 off-axis deformation (and, consequently, localized weakening), represented by rings of increased strain rate
333 ring around the ridge (see Sup. Fig. S1). Albeit on a different geodynamic setting, this observation is in
334 accordance with the works of Whattam and Stern (2015) and Stern and Dumitru (2019) on plume-induced
335 subduction initiation. In these works, the authors show that the edges of a plume induce a deformation ring
336 at the surface, along which new subduction zones can be triggered. Accordingly, the stress induced along
337 by the edges of mantle plumes is likely compressive, the opposite of the extensional conditions required for
338 any rift to be formed. When this factor is combined with the lack of far-field tectonic forcing in Model 3,
339 the only extensional stress present derives from the thermal upwelling at the ridge. Ultimately, this is likely
340 the reason behind the observed re-establishing of the MAR at its initial position in this model.

341 By contrast, all models in which the shift in global strain rate regime was simulated show the incipient
342 formation of a new transtensional site (Fig. 7B and C), with the NW-SE oriented shear zone acting as a
343 plate boundary which connects the MAR to the GF. As previously shown, the encroachment of the plume
344 head alone is sufficient (albeit with minor effects) to induce deformation in the lithosphere surrounding the
345 MAR. When this is coupled with the NE-SW extension imposed by the regional strain field (as illustrated
346 in Fig. 3), all requirements for a ridge jump are present. However, the formation of an transtensional shear
347 boundary with NW-SE orientation (i.e., similar to the Terceira Rift) can be formed simply by the shift in
348 tectonic forcing. This, therefore, not only begs the question of what the contribution of the plume to the
349 evolution of this system is; but also of how much of the observed deformation can be attributed to this
350 feature. One way to assess this is by comparing the results between models with and without a mantle
351 plume while maintaining the remaining features (i.e., Fig. 7B and C vs Fig. 6 and 4, respectively). In both
352 cases – with and without Azores Plateau – the values observed for the strain rate in the Azores domain are
353 higher under the influence of the plume. Not just this, but the absence of the plateau causes a significant
354 drop in the definition of the new shear zone and complete disappearance of the triangular Azores low
355 strain domain (corresponding to a relatively stronger block, compare in Fig. 7C vs 4D). We argue that, in
356 both cases, the increased strain rate within the Azores domain is the result of plume-induced deformation,
357 with the impingement of the plume head causing an upwards deflection (i.e., bulging) of the lithosphere
358 (Burov and Guillou-Frottier, 2005) and increased deformation at the surface (Wang, 2021). This is further

359 reinforced by the relatively confined nature of this strain rate increase, as it is limited to the new Azores
360 domain (Fig. 7B-D) and above the injection spot (Fig. 2). Despite its ability to localize strain along its
361 edges, the interior of the Azores Plateau also contributes towards delocalization when under the effect of an
362 encroaching mantle plume, albeit at a lower rate than standard oceanic lithosphere. As the plume impinges
363 on the base of the lithosphere, it produces a large thermal anomaly, gradually heating up the lithosphere of
364 the plateau, reducing its effective strength. With this decreased strength, the localization effect observed in
365 previous models (e.g., Fig. 4) is less efficient, resulting in an overall more diffuse higher strain rate within the
366 plateau. We suggest that this diffuse straining of the Azores Plateau, induced by lithosphere upwelling and
367 the plume-derived thermal anomaly, could provide an explanation for the uncertainty regarding the exact
368 location of the boundary between Nubia and Eurasia in this region (e.g., Marques et al., 2013; Fernandes
369 et al., 2006).

370 There is one additional effect that can be gleaned from comparing the plume models with and without
371 the Azores Plateau, which could be relevant for the evolution of the Azores system. As discussed previously,
372 when the plateau is present, there is a strong strain localization effect along its edges due to the existence
373 of rheological boundaries. By contrast, its absence promotes the existence of the diffuse high strain region.
374 Thus, we can infer from these results that it is likely that a growing plateau would induce the migration of
375 the deformation towards its edges. Thus, and as the formation of the Azores Plateau was not a single event
376 but instead spread over several magmatic phases over ca. 10 Ma (e.g., Beier et al., 2022), its growth led to
377 the systematic migration of the active deformation sites following its edges. At an early stage (ca. 10 Ma),
378 as the motion between Eurasia and Nubia shifts and induces the present-day right-lateral motion (Potter
379 and Szatmari, 2009; Rosenbaum et al., 2002), the Azores Plateau is represented by a small crustal thickening
380 close to the MAR. As the stress field rotated during this period, the first NW-SE extensional features are
381 formed, such as the Princess Alice Rift and minor volcanic edifices at the SE edge of the plateau. Over
382 time, as the plateau grows and the crustal thickening becomes more widespread, these extensional features
383 become inactive and most of the deformation concentrates along the NE edge of the plateau (Fig. 8B). We
384 argue that these events are a reflection of the strain localization effects observed in the models with the
385 Azores Plateau (both with and without mantle plumes) and can provide an explanation for the observed
386 changes in the plate boundary in this region (e.g., Neves et al., 2013).

387 5. Conclusions

388 With this numerical modelling work, we aimed to explore how the complex interaction between a ridge-
389 plume-transform system and the right-lateral motion between Eurasia and Nubia led to the opening of the
390 Terceira Rift and the gradual shift from a R-R-T to a diffuse R-R-R triple junction.

391 Our results suggest that the principal mechanism controlling the formation and extension of the Terceira
392 Rift (and other NW-SE oriented features) is the change in tectonic forcing imposed by the change in motion
393 between Eurasia and Nubia during the Early Miocene, acting in tandem with the strain localization effects
394 of the Azores Plateau. The shift towards a relative right-lateral motion between these plates induced a
395 rotation of the local stress field, promoting the localization of transtensional shear along the edges of the
396 plateau which, eventually, evolves into the Terceira Rift. Furthermore, under our modelling conditions,
397 the plume-ridge-transform interaction results in the establishment of a diffusively strained Azores domain,
398 where no distinct plate boundary can be defined. This is in-line with the presently uncertain/indistinct
399 plate boundary between Eurasia and Nubia in the Azores.

400 Overall, and considering the broader tectonic implications, our models suggest that these plume-ridge-
401 transform systems should not be interpreted as isolated systems, as they are strongly influenced by the
402 tectonic setting in which they occur. In natural systems, any ridge-plume system will be under a constant
403 far-field forcing, imposed by the tectonic setting at stake, which will control the orientation and distribution
404 of any geometric reorganization which is forced due to the plume-induced MAR disruption. There are over
405 20 possible configurations of triple junctions and more than 100 examples on Earth today (Cronin, 1992).
406 However, only a few have been studied with the depths of the Azores. Understanding how the Azores is
407 evolving thus provides a unique opportunity to understand how triple junction evolve. In particular, because
408 they are unstable and sensitive to large-scale plate reorganization. Furthermore, intra-oceanic rifts, such as
409 the Terceira Rift, are rare and have important implications for the evolution of Earth-like plate tectonics.
410 Understanding how they nucleate and evolve are also of key importance. In this case, the new rift seems
411 to have formed as the result of the interaction of a plume with a triple-junction during an episode of plates
412 reorganization.

413 From this, we hope that future works aim to explore this problematic in other plume-ridge-transform
414 triple junction sites, such as the Galapagos, as well as assess how a growing oceanic plateau could impact the
415 evolution of these systems. Such work will be fundamental in understanding how the everchanging changing
416 global tectonic settings influence the evolution of oceanic basins.

6. Acknowledgments

This work was funded by the Portuguese Fundação para a Ciência e a Tecnologia (FCT) I.P./MCTES through projects GEMMA (<https://doi.org/10.54499/PTDC/CTA-GEO/2083/2021>) and through national funds (PIDDAC) – UID/50019/2025 and LA/P/0068/2020 (<https://doi.org/10.54499/LA/P/0068/2020>).

7. Credit statement

Conceptualization: JA, JD, FR, RR, RF; **Data curation:** JA, JD, FR, RR, RF; **Formal analysis:** JA, JD, FR, RR, RF; **Funding acquisition:** RF; **Investigation:** JA, JD, FR, RR, RF; **Methodology:** JA, JD, FR, RR, RF; **Project administration:** RF; **Validation:** JA; **Visualization:** JA; **Writing – original draft:** JA, RF; **Writing – review & editing:** JA, JD, FR, RR, RF

References

- Albers, M., Christensen, U.R., 2001. Channeling of plume flow beneath mid-ocean ridges. Technical Report 1-2. URL: www.elsevier.com/locate/eps1, doi:10.1016/S0012-821X(01)00276-X.
- Arnould, M., Ganne, J., Coltice, N., Feng, X., 2019. Northward drift of the Azores plume in the Earth's mantle. *Nature Communications* 10, 1–8. URL: <http://dx.doi.org/10.1038/s41467-019-11127-7>, doi:10.1038/s41467-019-11127-7.
- Beier, C., Genske, F., Hübscher, C., Haase, K.M., Bach, W., Nomikou, P., 2022. The submarine Azores Plateau: Evidence for a waning mantle plume? *Marine Geology* 451, 106858. URL: <https://linkinghub.elsevier.com/retrieve/pii/S0025322722001293>, doi:10.1016/j.margeo.2022.106858.
- Bowin, C., Thompson, G., Schilling, J.G., 1984. Residual geoid anomalies in Atlantic Ocean Basin: Relationship to mantle plumes. *Journal of Geophysical Research: Solid Earth* 89, 9905–9918. URL: <https://agupubs.onlinelibrary.wiley.com/doi/10.1029/JB089iB12p09905>, doi:10.1029/JB089iB12p09905.
- Burov, E., Guillou-Frottier, L., 2005. The plume head-continental lithosphere interaction using a tectonically realistic formulation for the lithosphere. *Geophysical Journal International* 161, 469–490. URL: <https://dx.doi.org/10.1111/j.1365-246X.2005.02588.x>, doi:10.1111/j.1365-246X.2005.02588.x.
- Calignano, E., Sokoutis, D., Willingshofer, E., Gueydan, F., Cloetingh, S., 2015. Strain localization at the margins of strong lithospheric domains: Insights from analog models. *Tectonics* 34, 396–412. doi:10.1002/2014TC003756.
- Coltice, N., G erault, M., Ulyrova, M., 2017. A mantle convection perspective on global tectonics. *Earth-Science Reviews* 165, 120–150. URL: <https://linkinghub.elsevier.com/retrieve/pii/S0012825216304354><http://dx.doi.org/10.1016/j.earscirev.2016.11.006>, doi:10.1016/j.earscirev.2016.11.006.
- Cronin, V.S., 1992. Types and kinematic stability of triple junctions. *Tectonophysics* 207, 287–301. doi:10.1016/0040-1951(92)90391-I.
- DeMets, C., Gordon, R.G., Argus, D.F., 2010. Geologically current plate motions. *Geophysical Journal International* 181, 1–80. URL: <http://gji.oxfordjournals.org/cgi/doi/10.1111/j.1365-246X.2009.04491.x>, doi:10.1111/j.1365-246X.2009.04491.x.
- Drucker, D.C., Prager, W., 1952. Soil Mechanics and Plastic Analysis or Limit Design. *Quarterly of Applied Mathematics* 10, 157–165. doi:10.1090/qam/48291.
- Duarte, J., Rosas, F.M.F., Terrinha, P., Schellart, W.W.P., Boutelier, D., Gutscher, M.A.M.A.M.A., Ribeiro, A., 2013. Are subduction zones invading the atlantic? Evidence from the southwest iberia margin. *Geology* 41, 839–842. doi:10.1130/G34100.1.
- Fernandes, R.M., Ambrosius, B.A., Noomen, R., Bastos, L., Wortel, M.J., Spakman, W., Govers, R., 2003. The relative motion between Africa and Eurasia as derived from ITRF2000 and GPS data. *Geophysical Research Letters* 30, 1–5. doi:10.1029/2003GL017089.
- Fernandes, R.M., Bastos, L., Miranda, J.M., Lourenço, N., Ambrosius, B.A., Noomen, R., Simons, W., 2006. Defining the plate boundaries in the Azores region. *Journal of Volcanology and Geothermal Research* 156, 1–9. doi:10.1016/j.jvolgeores.2006.03.019.
- Fernandes, R.M.S., Bastos, L., Ambrosius, B.A.C., Noomen, R., Matheussen, S., Baptista, P., 2004. Recent Geodetic Results in the Azores Triple Junction Region, in: *Geodynamics of Azores-Tunisia*. Birkh user Basel, Basel, pp. 683–699. URL: http://link.springer.com/10.1007/978-3-0348-7899-9_12, doi:10.1007/978-3-0348-7899-9_12.
- Gente, P., Dyment, J., Maia, M., Goslin, J., 2003. Interaction between the Mid-Atlantic Ridge and the Azores hot spot during the last 85 Myr: Emplacement and rifting of the hot spot-derived plateaus. *Geochemistry, Geophysics, Geosystems* 4. doi:10.1029/2003GC000527.

468 Georgen, J.E., Lin, J., 2002. Three-dimensional passive flow and temperature structure beneath oceanic ridge-ridge-ridge triple
469 junctions. *Earth and Planetary Science Letters* 204, 115–132. URL: [https://linkinghub.elsevier.com/retrieve/pii/
470 S0012821X02009536](https://linkinghub.elsevier.com/retrieve/pii/S0012821X02009536), doi:10.1016/S0012-821X(02)00953-6.

471 Georgen, J.E., Sankar, R.D., 2010. Effects of ridge geometry on mantle dynamics in an oceanic triple junction region: Impli-
472 cations for the Azores Plateau. *Earth and Planetary Science Letters* 298, 23–34. doi:10.1016/j.epsl.2010.06.007.

473 Gibson, S.A., Geist, D.J., Richards, M.A., 2015. Mantle plume capture, anchoring, and outflow during Galápagos plume-ridge
474 interaction. *Geochemistry, Geophysics, Geosystems* 16, 1634–1655. URL: [https://agupubs.onlinelibrary.wiley.com/doi/
475 10.1002/2015GC005723](https://agupubs.onlinelibrary.wiley.com/doi/10.1002/2015GC005723), doi:10.1002/2015GC005723.

476 Hensen, C., Duarte, J.C., Vannucchi, P., Mazzini, A., Lever, M.A., Terrinha, P., Géli, L., Henry, P., Villinger, H., Morgan,
477 J., Schmidt, M., Gutscher, M.A., Bartolome, R., Tomonaga, Y., Polonia, A., Gràcia, E., Tinivella, U., Lupi, M., Çağatay,
478 M.N., Elvert, M., Sakellariou, D., Matias, L., Kipfer, R., Karageorgis, A.P., Ruffine, L., Liebetrau, V., Pierre, C., Schmidt,
479 C., Batista, L., Gasperini, L., Burwicz, E., Neres, M., Nuzzo, M., 2019. Marine transform faults and fracture zones: A joint
480 perspective integrating seismicity, fluid flow and life. *Frontiers in Earth Science* 7, 1–29. doi:10.3389/feart.2019.00039.

481 Jain, C., Korenaga, J., 2020. Synergy of Experimental Rock Mechanics, Seismology, and Geodynamics Reveals Still Elusive
482 Upper Mantle Rheology. *Journal of Geophysical Research: Solid Earth* 125, e2020JB019896. URL: [https://doi.org/10.,
483 doi:10.1029/2020JB019896](https://doi.org/10.1029/2020JB019896).

484 Jolivet, L., Faccenna, C., 2000. Mediterranean extension and the Africa-Eurasia collision. *Tectonics* 19, 1095–1106. URL:
485 <https://agupubs.onlinelibrary.wiley.com/doi/10.1029/2000TC900018>, doi:10.1029/2000TC900018.

486 Kaus, B.J.P., Popov, A.A., Baumann, T.S., Pusok, A.E., Bauville, A., Fernandez, N., Collignon, M., 2016. Forward and Inverse
487 Modelling of Lithospheric Deformation on Geological Timescales. *NIC Series* 48, 978–3.

488 Keppler, R., Rosas, F., Nagel, T., 2013. Thin viscous middle-crust and evolving fault distribution during continental rifting:
489 Insights from analog modeling experiments. *Tectonophysics* 608, 161–175. URL: [http://dx.doi.org/10.1016/j.tecto.
490 2013.10.001](http://dx.doi.org/10.1016/j.tecto.2013.10.001), doi:10.1016/j.tecto.2013.10.001.

491 Kidd, R.B., Searle, R.C., Ramsay, A.T., Prichard, H., Mitchell, J., 1982. The geology and formation of King’s Trough, northeast
492 Atlantic Ocean. *Marine Geology* 48, 1–30. URL: [https://linkinghub.elsevier.com/retrieve/pii/002532278290127X,
493 doi:10.1016/0025-3227\(82\)90127-X](https://linkinghub.elsevier.com/retrieve/pii/002532278290127X).

494 King, S.D., 2016. Reconciling laboratory and observational models of mantle rheology in geodynamic modelling. *Journal of
495 Geodynamics* 100, 33–50. doi:10.1016/j.jog.2016.03.005.

496 Lourenço, N., Miranda, J.M., Luis, J.F., Ribeiro, A., Mendes Victor, L.A., Madeira, J., Needham, H.D., 1998. Morpho-
497 tectonic analysis of the Azores Volcanic Plateau from a new bathymetric compilation of the area. Technical Report 3.
498 doi:1004505401547.

499 Luis, J.F., Miranda, J.M., 2008. Reevaluation of magnetic chrons in the North Atlantic between 35°N and 47°N: Implications
500 for the formation of the Azores Triple Junction and associated plateau. *Journal of Geophysical Research: Solid Earth* 113.
501 doi:10.1029/2007JB005573.

502 Luis, J.F., Miranda, J.M., Galdeano, A., Patriat, P., 1998. Constraints on the structure of the Azores spreading center from
503 gravity data. *Marine Geophysical Research* 20, 157–170. doi:10.1023/A:1004698526004.

504 Lynch, H.D., Morgan, P., 1987. The tensile strength of the lithosphere and the localization of extension. *Geological Society
505 Special Publication* 28, 53–65. doi:10.1144/GSL.SP.1987.028.01.05.

506 Mackwell, S.J., Zimmerman, M.E., Kohlstedt, D.L., 1998. High-temperature deformation of dry diabase with application to
507 tectonics on Venus. *Journal of Geophysical Research: Solid Earth* 103, 975–984. URL: [https://agupubs.onlinelibrary.
508 wiley.com/doi/full/10.1029/97JB02671](https://agupubs.onlinelibrary.wiley.com/doi/full/10.1029/97JB02671)<https://agupubs.onlinelibrary.wiley.com/doi/abs/10.1029/97JB02671><https://agupubs.onlinelibrary.wiley.com/doi/10.1029/97JB02671>, doi:10.1029/97jb02671.

509 Madeira, J., 1998. Estudos de neotectónica nas ilhas do Faial, Pico e S.” Jorge: Uma Contribuição para o Conhecimento
510 Geodinâmico da Junção Tripla dos Açores. Doctorate thesis. University of Lisbon.

511 Madeira, J., Ribeiro, A., 1990. Geodynamic models for the Azores triple junction: A contribution from tectonics. *Tectonophysics*
512 184, 405–415. URL: <https://linkinghub.elsevier.com/retrieve/pii/004019519090452E>, doi:10.1016/0040-1951(90)
513 90452-E.

514 Manglik, A., Christensen, U.R., 2006. Effect of lithospheric root on decompression melting in plume - Lithosphere interaction
515 models. *Geophysical Journal International* 164, 259–270. doi:10.1111/j.1365-246X.2005.02811.x.

516 Marques, F.O., Catalão, J.C., DeMets, C., Costa, A.C., Hildenbrand, A., 2013. GPS and tectonic evidence for a diffuse plate
517 boundary at the Azores Triple Junction. *Earth and Planetary Science Letters* 381, 177–187. URL: [http://dx.doi.org/10.
518 1016/j.epsl.2013.08.051](http://dx.doi.org/10.1016/j.epsl.2013.08.051), doi:10.1016/j.epsl.2013.08.051.

519 Miranda, J.M., Luis, J.F., Lourenço, N., Fernandes, R.M., 2015. The structure of the Azores Triple Junction: Implications for
520 São Miguel Island. *Geological Society Memoir* 44, 5–13. doi:10.1144/M44.2.

521 Mittelstaedt, E., Ito, G., van Hunen, J., 2011. Repeat ridge jumps associated with plume-ridge interaction, melt transport,
522 and ridge migration. *Journal of Geophysical Research* 116, B01102. URL: [http://doi.wiley.com/10.1029/2010JB007504,
523 doi:10.1029/2010JB007504](http://doi.wiley.com/10.1029/2010JB007504).

524 Neves, M.C., Miranda, J.M., Luis, J.F., 2013. The role of lithospheric processes on the development of linear vol-
525 canic ridges in the Azores. *Tectonophysics* 608, 376–388. URL: [https://www.sciencedirect.com/science/article/pii/
526 S0040195113005726](https://www.sciencedirect.com/science/article/pii/S0040195113005726), doi:10.1016/j.tecto.2013.09.016.

527 Pang, F., Liao, J., Ballmer, M.D., Li, L., 2023. Plume-ridge interactions: Ridgeward versus plate-drag plume flow. *Solid Earth*
528 14, 353–368. doi:10.5194/se-14-353-2023.

529 Piccolo, A., Kaus, B.J., White, R.W., Palin, R.M., Reuber, G.S., 2020. Plume — Lid interactions during the Archean and
530 implications for the generation of early continental terranes. *Gondwana Research* 88, 150–168. URL: [https://doi.org/10.
531 1016/j.gr.2020.06.024](https://doi.org/10.1016/j.gr.2020.06.024), doi:10.1016/j.gr.2020.06.024.

- 533 Pilidou, S., Priestley, K., Debayle, E., Gudmundsson, Ó., 2005. Rayleigh wave tomography in the North Atlantic: High
534 resolution images of the Iceland, Azores and Eifel mantle plumes. *Lithos* 79, 453–474. doi:10.1016/j.lithos.2004.09.012.
- 535 Potter, P.E., Szatmari, P., 2009. Global Miocene tectonics and the modern world. *Earth-Science Reviews* 96, 279–295. URL:
536 <http://dx.doi.org/10.1016/j.earscirev.2009.07.003>, doi:10.1016/j.earscirev.2009.07.003.
- 537 Püthe, C., Gerya, T., 2014. Dependence of mid-ocean ridge morphology on spreading rate in numerical 3-D models. *Gondwana*
538 *Research* 25, 270–283. doi:10.1016/j.gr.2013.04.005.
- 539 Ranalli, G., 1997. Rheology and deep tectonics. URL: <http://www.earth-prints.org/handle/2122/1523>, doi:10.4401/
540 [ag-3893](http://www.earth-prints.org/handle/2122/1523).
- 541 Ribe, N., Christensen, U., Theiβing, J., 1995. The dynamics of plume-ridge interaction, 1: Ridge-centered plumes. *Earth*
542 *and Planetary Science Letters* 134, 155–168. URL: <https://linkinghub.elsevier.com/retrieve/pii/S0012821X9500116T>,
543 doi:10.1016/0012-821X(95)00116-T.
- 544 Rosenbaum, G., Lister, G.S., Duboz, C., 2002. Relative motions of Africa, Iberia and Europe during Alpine orogeny.
545 *Tectonophysics* 359, 117–129. URL: <https://linkinghub.elsevier.com/retrieve/pii/S0040195102004420>, doi:10.1016/
546 [S0040-1951\(02\)00442-0](https://linkinghub.elsevier.com/retrieve/pii/S0040195102004420).
- 547 Schettino, A., Macchiavelli, C., 2016. Plate kinematics of the central Atlantic during the Oligocene and early Miocene.
548 *Geophysical Journal International* 205, 408–426. doi:10.1093/gji/ggw022.
- 549 Schilling, J.G., 1991. Fluxes and excess temperatures of mantle plumes inferred from their interaction with migrating mid-ocean
550 ridges. *Nature* 352, 397–403. URL: <https://www.nature.com/articles/352397a0>, doi:10.1038/352397a0.
- 551 Silveira, G., Stutzmann, E., Davaille, A., Montagner, J.P., Mendes-Victor, L., Sebai, A., 2006. Azores hotspot signature in the
552 upper mantle. *Journal of Volcanology and Geothermal Research* 156, 23–34. doi:10.1016/j.jvolgeores.2006.03.022.
- 553 Srivastava, S.P., Schouten, H., Roest, W.R., Klitgord, K.D., Kovacs, L.C., Verhoef, J., Macnab, R., 1990. Iberian plate
554 kinematics: a jumping plate boundary between Eurasia and Africa. *Nature* 344, 756–759. URL: [https://www.nature.com/
555 articles/344756a0](https://www.nature.com/articles/344756a0), doi:10.1038/344756a0.
- 556 Stern, R.J., Dumitru, T.A., 2019. Eocene initiation of the Cascadia subduction zone: A second example of plume-induced
557 subduction initiation? *Geosphere* 15, 659–681. doi:10.1130/GES02050.1.
- 558 Storch, B., Haase, K.M., Romer, R.H.W., Beier, C., Koppers, A.A.P., 2020. Rifting of the oceanic Azores Plateau with
559 episodic volcanic activity. *Scientific Reports* 10, 19718. URL: <https://www.nature.com/articles/s41598-020-76691-1>,
560 doi:10.1038/s41598-020-76691-1.
- 561 Sun, W., Langmuir, C.H., Ribe, N.M., Zhang, L., Sun, S., Li, H., Li, C., Fan, W., Tackley, P.J., Sanan, P., 2021. Plume-ridge
562 interaction induced migration of the Hawaiian-Emperor seamounts. *Science Bulletin* 66, 1691–1697. doi:10.1016/j.scib.
563 [2021.04.028](https://www.nature.com/articles/s41598-020-76691-1).
- 564 Vogt, P.R., Jung, W.Y., 2004. The Terceira Rift as hyper-slow, hotspot-dominated oblique spreading axis: A comparison
565 with other slow-spreading plate boundaries. *Earth and Planetary Science Letters* 218, 77–90. doi:10.1016/S0012-821X(03)
566 [00627-7](https://www.nature.com/articles/S0012-821X(03)00627-7).
- 567 Wang, K., 2021. If not brittle: Ductile, plastic, or viscous? *Seismological Research Letters* 92, 1181–1184. doi:10.1785/
568 [0220200242](https://www.seismology.org/doi/10.1785/SRLE-2020-0242).
- 569 Weiß, B.J., Hübscher, C., Lüdmann, T., 2015. The tectonic evolution of the southeastern Terceira Rift/São Miguel region
570 (Azores). *Tectonophysics* 654, 75–95. URL: <https://www.sciencedirect.com/science/article/pii/S0040195115002437>,
571 doi:10.1016/j.tecto.2015.04.018.
- 572 Whattam, S.A., Stern, R.J., 2015. Late Cretaceous plume-induced subduction initiation along the southern margin of the
573 Caribbean and NW South America: The first documented example with implications for the onset of plate tectonics.
574 *Gondwana Research* 27, 38–63. URL: <http://dx.doi.org/10.1016/j.gr.2014.07.011>, doi:10.1016/j.gr.2014.07.011.
- 575 Whittaker, J.M., Afonso, J.C., Masterton, S., Müller, R.D., Wessel, P., Williams, S.E., Seton, M., 2015. Long-term interaction
576 between mid-ocean ridges and mantle plumes. *Nature Geoscience* 8, 479–483. doi:10.1038/NGE02437.
- 577 Willis, K., Houseman, G.A., Evans, L., Wright, T., Hooper, A., 2019. Strain localization by shear heating and the development
578 of lithospheric shear zones. *Tectonophysics* 764, 62–76. URL: <https://doi.org/10.1016/j.tecto.2019.05.010>, doi:10.
579 [1016/j.tecto.2019.05.010](https://doi.org/10.1016/j.tecto.2019.05.010).
- 580 Yang, T., Shen, Y., van der Lee, S., Solomon, S.C., Hung, S.H., 2006. Upper mantle structure beneath the Azores hotspot from
581 finite-frequency seismic tomography. *Earth and Planetary Science Letters* 250, 11–26. doi:10.1016/j.epsl.2006.07.031.

582 Appendix A. Model limitations

583 The presented models aim to explore how the Azores system may have been shaped by the complex
584 interactions between a mantle plume, the MAR and the relative motions between Eurasia and Nubia.
585 However, as with most models, any conclusion drawn must take into consideration the limitations of the
586 methodology.

587 One of the limitations pertains to an existing uncertainty in the rheology of the upper mantle (e.g.,
588 [King, 2016](#); [Jain and Korenaga, 2020](#), and references therein). While there is some variability on the choice
589 of rheological parameters (e.g., [Table S1](#)), it should be expected that slight variations of these parameters
590 could lead to different results. For instance, a change in the viscosity of the ascending plume materials could
591 result in the faster or slower ascent through the mantle, or even on determining the formation of a narrower
592 vs. wider plume head.

593 On the topic of mantle plumes, there is another degree of uncertainty regarding the position of the Azores
594 plume, specifically concerning the location of the stem in the past and the exact root depth of the plume
595 itself (e.g., [Gente et al., 2003](#); [Silveira et al., 2006](#); [Yang et al., 2006](#)). Given this uncertainty, our selection
596 of injection spot represents a compromise that may ultimately influence the evolution of our models, as a
597 more distant injection of the plume would likely result in a different outcome.

598 Additionally, under our modelling setup, no two-phase flow is included. Mantle plumes are known
599 to induce partial melting within the lithosphere (e.g., [Manglik and Christensen, 2006](#)), which not only
600 introduces a liquid phase into the system but also weakens the local rheology (e.g., [Whattam and Stern,](#)
601 [2015](#)). As stated before, a weaker rheology of the Azores Plateau directly causes a wider distribution of
602 the strain in this domain. It is likely that by adopting two-phase flow this effect would be more impactful,
603 which suggests that our results might represent an underestimation of the strain rate in the Azores.

604 Furthermore, there are also some limitations regarding the initial geometry for the Azores domain used
605 for the initial setup. As stated previously, the initial geometry selected for this study was based on the plate
606 reconstructions for the Azores domain during the Early Miocene (e.g., [Madeira, 1998](#); [Gente et al., 2003](#);
607 [Miranda et al., 2015](#)). However, there is a degree of uncertainty on any reconstruction that may influence
608 the way through which the system will evolve. Furthermore, we assume a relatively uniform composition of
609 the oceanic plates in our models, with no smaller scale features (such as individual formations and/or earlier
610 fractures). While we expect these individual second-order features to not significantly contribute to the
611 outcome of the models, their collective behaviour may contribute towards the degree of strain localization.

612 Another limitation is the rheology of the prescribed weak zones to simulate the fracture zones and the

613 transform faults, all of which have been designed as being isoviscous (i.e., constant Newtonian viscosity)
614 regions. In nature, fracture/fault zones are heterogeneous with a complex mixture of blocks and gouge
615 which, when the stress is dropped, inevitably are cemented together to form a consistent lithology. In order
616 to accurately replicate this type of complex rheology it is important to apply extremely fine resolutions on
617 top of these features. As our objective was to simulate how a weak zone could influence the development
618 of a new transtensional boundary, and not specifically simulate the dynamics of fault zones, as well due to
619 computer power limitations to include such heterogeneities, we have adopted this simplification of assuming
620 isoviscous rheologies.

621 Finally, regarding the choice of boundary conditions which usually consist of adopted kinematic im-
622 positions with the aim to replicate natural dynamics. For instance, although natural mid-ocean ridges are
623 mostly driven by (far-field) slab-pull, ridge-push and mantle convection forces (e.g., [Coltice et al., 2017](#)),
624 non-whole Earth models simulate the formation and evolution of these features by either directly impose
625 known kinematic conditions (e.g., [Georgen and Lin, 2002](#)) or derive them from regional strain rates (e.g.,
626 [Pütke and Gerya, 2014](#)). While this simplification changes the effective forces in the system (e.g., removing
627 the compression imposed by an opening ridge), it is a forceful one due to the computation power required
628 to simulate the entire Earth system when compared to the study of a small region such as the Azores Triple
629 Junction.

630 **Appendix B. Complete set of modelling parameters**

Table S1: Physical parameters applied in the models, for each of the different phases. The softening parameters are found in Methods section. The two values for density in the Oceanic crust column represent the plateau and general oceanic domains, respectively.

Properties	Parameters	Oceanic Crust	Weak zones	Mantle plume	Upper Mantle
Density	ρ_0 - kg/m ³	3260 / 3300	3300	3300	3300
Dislocation creep	B_n - Pa ⁻ⁿ /s ⁻¹	8	-	2.50x10 ⁴	2.50x10 ⁴
	n	4.7	-	3.5	3.5
	E_n - J/MPa/mol	4.85x10 ⁵	-	5.30x10 ⁴	5.30x10 ⁴
	V_n - m ³ /mol	0	-	1.35x10 ⁻⁵	1.35x10 ⁻⁵
Diffusion creep	B_I - Pa ⁻ⁿ /s ⁻¹	-	-	1.50x10 ⁹	1.50x10 ⁹
	n	-	-	1	1
	E_I - J/MPa/mol	-	-	3.75x10 ⁵	3.75x10 ⁵
	V_I - m ³ /mol	-	-	1.35x10 ⁻⁵	1.35x10 ⁻⁵
Plastic flow	Cohesion - MPa	30	10	30	30
	Softened cohesion - MPa	0.3	-	-	0.3
	ϕ - degrees	0.1	15	20	20
	Softened ϕ - degrees	0.001	0.068	-	0.2
Elasticity	G - Pa	5.00x10 ¹⁰	5.00x10 ¹⁰	5.00x10 ¹⁰	5.00x10 ¹⁰
Thermal properties	Expansivity (α) - 1/K	3x10 ⁻⁵	3x10 ⁻⁵	3x10 ⁻⁵	3x10 ⁻⁵
	Conductivity (κ) - W/m/k	3	3	3	3
	Heat capacity - J/kg/K	1050	1050	1050	1050

Model 3

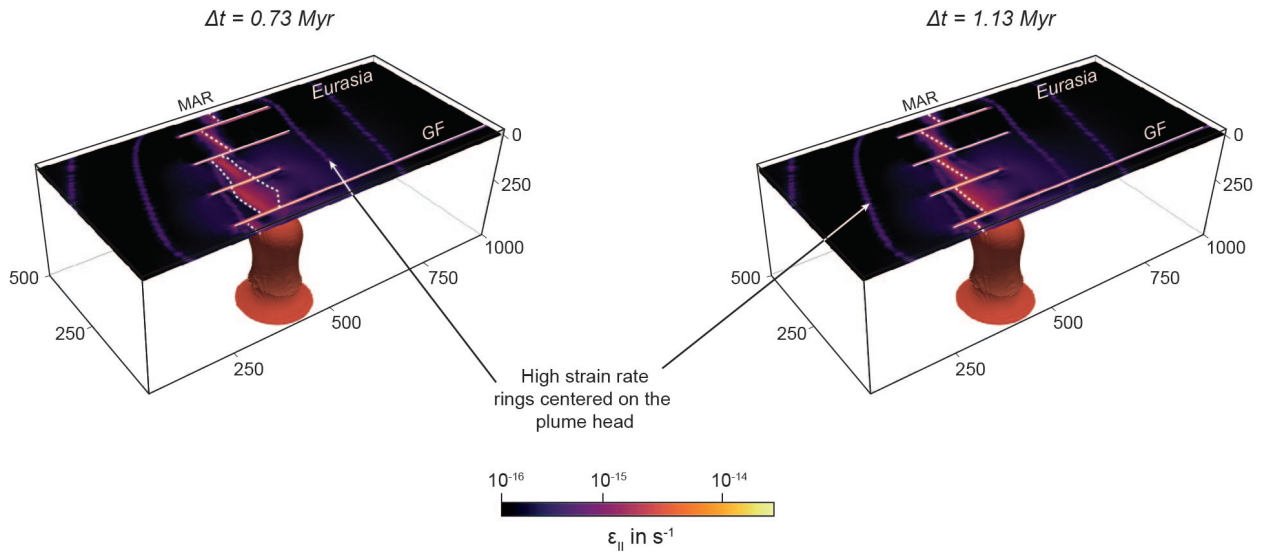


Figure S1: **Model 3 with a narrower strain rate colouring.** By observing Model 3 with a narrower range of strain rate values (compare with the ones in Fig. 7A) it is possible to observe the higher strain rate rings centred on the plume head, signalling its impact on the oceanic lithosphere above.